Fermi National Accelerator Laboratory

FERMILAB-Pub-93/315-E

T861

Search for Antiproton Decay at the Fermilab Antiproton Accumulator

S. Geer, J. Marriner, R. Ray and J. Streets

Fermi National Accelerator Laboratory
P.O. Box 500, Batavia, Illinois 60510

M. Lindgren, Th. Muller, J. Quackenbush

University of California
Los Angeles, California 90024-1547

T. Armstrong

Pennsylvania State University
University Park, Pennsylvania 16802

November 1993

Submitted to *Physical Review Letters*

Operated by Universities Research Association Inc. under Contract No. DE-AC02-76CHO3000 with the United States Department of Energy

Disclaimer

FERMILAB-PUB-93/315-E

October, 1993

SEARCH FOR ANTIPROTON DECAY AT THE FERMILAB ANTIPROTON ACCUMULATOR

S. Geer, J. Marriner, R. Ray, J. Streets
Fermi National Accelerator Laboratory, Batavia, Illinois 60510

M. Lindgren, Th. Muller, J. Quackenbush.
University of California, Los Angeles, California 90024-1547

T. Armstrong
Pennsylvania State University, University Park, Pennsylvania 16802

(T861 Collaboration)

ABSTRACT

A search for antiproton decay has been made at the Fermilab antiproton accumulator. Limits are placed on five antiproton decay modes. At the 95% C.L. we find that $\tau_{\bar{p}}$ /BR($\bar{p} \rightarrow e^- \gamma$) > 1848 years, $\tau_{\bar{p}}$ /BR($\bar{p} \rightarrow e^- \pi^0$) > 554 years, $\tau_{\bar{p}}$ /BR($\bar{p} \rightarrow e^- \eta$) > 171 years, $\tau_{\bar{p}}$ /BR($\bar{p} \rightarrow e^- K_S^0$) > 29 years, and $\tau_{\bar{p}}$ /BR($\bar{p} \rightarrow e^- K_L^0$) > 9 years.

PCACS numbers 11.30.Er, 13.30.Ce,14.20.Dh

Submitted to Physical Review Letters, October 25th, 1993.

There has been a considerable experimental effort devoted to the search for proton decay. As a result we know that the proton lifetime $\tau_p > O(10^{32})$ years[1]. The CPT theorem requires that the proton and $\bar{p}$ lifetimes are equal. A search for $\bar{p}$ decay with a short lifetime ($\tau_{\bar{p}} < \tau_p$) tests both the CPT theorem and the intrinsic stability of antimatter.

There have been a number of searches for the decay of antiprotons stored in ion traps[2] and storage rings[3]. The most stringent published limit, $\tau_{\bar{p}} > 3.4$ months[2], was obtained by setting a limit on the containment lifetime of ≈1000 antiprotons stored in an ion trap. In addition to these direct searches for $\bar{p}$ decay, cosmic ray experiments can search indirectly. The observation of cosmic ray antiprotons with rates consistent with secondary production in the interstellar medium would imply that $\gamma\tau_{\bar{p}} > T$, where γ is the Lorentz factor, and T is the $\bar{p}$ confinement time within the galaxy [$O(10^7$ years)]. Although earlier balloon experiments reported the observation of low energy antiprotons, a more recent experiment with greater sensitivity failed to observe a signal. One balloon experiment searching at higher $\bar{p}$ energies ($\gamma \geq 4$) has reported[4] the observation of cosmic ray antiprotons; however the experiment lacked particle identification and its ability to identify antiprotons has been questioned. Hence, there is no confirmed limit on $\tau_{\bar{p}}$ from cosmic ray experiments.

In this paper we describe a new search for $\bar{p}$ decay. The experiment was performed at the Fermilab antiproton accumulator, operating with a beam momentum of 8.9 GeV/c, beam currents in the range 20–30 mA (1 mA in the accumulator corresponds to 10^{10} stored antiprotons), and typical beam lifetimes of 300 hours. The detector was located downstream of a 15.9m straight section in the 474m circumference accumulator ring. The experimental setup (Fig. 1a) consisted of:

(i) A 5m long stainless steel vacuum pipe with an inner diameter of 3 inches and a wall thickness of 0.7 mm. The measured pressures at the upstream and downstream pipe ends were respectively $3^{+3.0}_{-1.5} \times 10^{-10}$ Torr and $8^{+8}_{-4} \times 10^{-11}$ Torr. A mass spectrometer

analysis of the residual gas showed the presence of H_2 (2×10^{-10} Torr), CH_4 (7×10^{-12} Torr), H_2O (4×10^{-11} Torr), CO (2×10^{-11} Torr), and CO_2 (1×10^{-11} Torr).

(ii) The forward electromagnetic calorimeter of the E760 experiment[5]. The calorimeter consists of 144 rectangular modules arranged in a 13×13 array with 6 modules at each of the 4 corners missing, and the central module absent to enable the beam pipe to pass through the calorimeter. Each module consists of 148 alternate layers of lead and acrylic scintillator plates with transverse dimensions of 10×10 cm^2. The lead plates are 1 mm thick. The first 32 scintillator plates are 0.64 cm thick, and the remaining 42 plates are alternately 0.64 cm and 0.32 cm thick. The active length of the module is 48.4 cm (17.7 radiation lengths). In response to electrons and photons, the calorimeter energy resolution is given by $\sigma/E = 0.2 / \sqrt{E[GeV]}$. The calorimeters linearity has been checked using 1 GeV and 3 GeV electron beams. In this energy range non-linearities do not exceed a few percent. The calorimeters response to neutrons and charged hadrons is less precise. The measured energies of these particles tends to be less than their real energies since most hadronic showers are not fully contained within the calorimeter.

(iii) Additional scintillation counters used to confirm that particles depositing energy in the calorimeter come predominantly from beam-gas interactions within the beampipe.

The calorimeter cells were grouped into six trigger sectors (Fig. 1b). The trigger required that the energy deposited in the sector with the largest energy deposition E_{TRIG} exceed a threshold value, which was adjusted within the range 1.5 – 2.5 GeV. Data were taken over a one week period during which the experiment recorded 6.8 million events. During data taking the beam current was monitored and the number of antiprotons $N_{\bar{p}}(t)$ determined to better than 1%. The number of stored antiprotons integrated over the live-time of the experiment was $\int N_{\bar{p}}(t)dt = (1.280 \pm 0.013) \times 10^8$ years. Offline, after

applying final calorimeter calibrations, the quantity E_{TRIG} was recalculated and events with $E_{TRIG} > 4$ GeV selected for further analysis. Two million events passed this requirement.

To compare event rates and properties with expectations for beam–gas interactions we have developed a Monte Carlo program which generates multi–pion final states for annihilation processes with up to 11 final state particles and non-annihilation processes with up to 9 final state particles. Coulomb scattering has been implemented taking into account the measured residual gas composition in the beampipe. The generator uses published measurements of exclusive, semi-inclusive, and topological cross-sections for $\bar{p}p$[6] and $\bar{p}n$[7] interactions at ≈ 8.9 GeV/c, and the measured kinematics for elastic scattering and for three-body non-annihilation final states. All other processes have been generated with a longitudinal phase space generator, with the particle mean transverse momenta adjusted to reproduce, as a function of final state multiplicity, the measured transverse momenta in annihilation and non-annihilation events. Beam-gas interactions were generated along the $\bar{p}$ orbit from 19m upstream to 1m downstream of the calorimeter, and the GEANT[8] Monte Carlo program used to track generated particles through the detector and simulate, as a function of particle type, the energy deposited in the calorimeter and the resulting calorimeter response.

The beam-gas Monte Carlo program predicts a trigger rate ($E_{TRIG} > 4$ GeV) of 55^{+55}_{-28} Hz when there are 2.6×10^{11} antiprotons in the accumulator, where the uncertainty on the prediction reflects the uncertainty on the vacuum inside the beam-pipe. The predicted rate is in good agreement with the measured rate of 72 Hz, which suggests that the recorded events originate predominantly from beam-gas interactions. After comparing the measured calorimeter energy distribution with the beam-gas Monte Carlo prediction, and fitting for the absolute calorimeter energy scale, we find that the Monte Carlo gives a reasonable description of the measured energy distribution (Fig. 2a), and the fit determines the energy scale to $\pm$ 2%. The Monte Carlo also describes the distribution of calorimeter cell energies

over an interval in which the rate falls by more than three orders of magnitude (Fig. 2b). To further compare the event characteristics with the Monte Carlo predictions we define:

a) The number of calorimeter clusters, N_C. The cluster finder forms a cluster by associating all cells within a 3×3 grid around the highest energy seed cell. Seed cells are defined as cells which have an energy $E_i > 50$ MeV, and have not been previously associated with a cluster. Clustering is repeated until no seed cells remain.

b) The energy imbalance, $S \equiv (E_X^2 + E_Y^2)^{1/2} / E_{TOT}$, where $E_X = \sum_i E_i x_i$, $E_Y = \sum_i E_i y_i$, E_{TOT} is the total calorimeter energy, and the i^{th} cell is located at position (x_i, y_i) with respect to the beam axis.

The Monte Carlo predictions for N_C and S give a reasonable description of the data (Fig. 3). We conclude that the recorded events arise predominantly from beam-gas interactions.

In contrast to the majority of the observed events, we would expect that two-body $\bar{p}$ decays in which both decay products deposit all of their energy in the calorimeter would result in well balanced events with two calorimeter clusters and $8 < E_{TOT} < 10$ GeV. As an example, in Fig. 4a the measured E_{TOT} distribution for events passing the loose energy balance requirement $S < 0.5$ is compared with the Monte Carlo prediction for $\bar{p} \rightarrow e^- \pi^0$ decay with $\tau_{\bar{p}} / BR(\bar{p} \rightarrow e^- \pi^0) = 3.4$ months. The data clearly exclude $\tau_{\bar{p}} / BR(\bar{p} \rightarrow e^- \pi^0) = 3.4$ months. The sensitivity of the search for $\bar{p} \rightarrow e^- \pi^0$ decay can be improved by requiring well balanced events ($S < 0.1$) with $N_C = 2$. Three events survive these cuts, of which only one event has $8 < E_{TOT} < 10$ GeV (Fig. 4b).

To extract a limit on $\bar{p} \rightarrow e^- \pi^0$ decay we consider the event with $N_C = 2$, $S < 0.1$, and $8 < E_{TOT} < 10$ GeV to be signal. Let the number of events passing the cuts be N, and the poisson upper limit on N be N_{MAX}. We have $N = 1$ and $N_{MAX} = 4.74$ (95% C.L.). The limit on $\tau_{\bar{p}} / BR$ is given by:

$$\tau_{\bar{p}}/BR \; > \; \frac{\varepsilon}{\gamma} \; \frac{1}{N_{MAX}} \; \int N_{\bar{p}}(t)dt \; ,$$

where the Lorentz factor $\gamma = 9.538 \pm 0.010$, and ε is the fraction of decays taking place uniformly around the accumulator ring that would pass the trigger and event selection requirements. The GEANT Monte Carlo has been used to simulate the detector response, and calculate ε. We find that $\varepsilon = (2.19 \pm 0.20 \pm 0.07) \times 10^{-4}$, where the first error is statistical and the second error reflects the uncertainty on ε due to the uncertainty on the calorimeter energy scale. To extract a conservative limit on $\tau_{\bar{p}}$ /BR we have added these two errors in quadrature and reduced ε by one standard deviation (1σ). As an additional check the event selection has been repeated with the calorimeter energy scale changed by $\pm 1\sigma$. When this is done, there is no increase in the number of events passing the selection cuts. Finally, we increase γ and decrease $N_{\bar{p}}(t)$ by 1σ. At the 95% C.L. we find that $\tau_{\bar{p}}$ /BR($\bar{p} \rightarrow e^- \pi^0$) > 554 years.

In addition to $\bar{p} \rightarrow e^- \pi^0$ there are several other two-body decay modes which would result in events with $S < 0.1$, $N_C = 2$, and $8 < E_{TOT} < 10$ GeV; namely $\bar{p} \rightarrow e^- X$, where $X = \gamma$, η, K^0_S, or K^0_L. The calculated ε for these four additional modes, together with the resulting lower limits on $\tau_{\bar{p}}$ /BR, are listed in Table 1. The most stringent limit is for the decay $\bar{p} \rightarrow e^- \gamma$. At the 95% C.L. we find that $\tau_{\bar{p}}/BR(\bar{p} \rightarrow e^- \gamma) > 1848$ years.

We thank the Fermilab Accelerator and Physics Division staff for their support and encouragement. We also wish to acknowledge the co-operation of the E760 collaboration which enabled us to use existing readout and data acquisition systems. This work was supported by the Department of Energy and the National Science Foundation.

[1] Particle Data Group; Phys, Rev. D45 (1992) Part II.

[2] G. Gabrielse et al; Phys. Rev. Lett. 65 (1990) 1317.

[3] M. Bregman et al; Phys. Lett. 78B (1978) 174; M. Bell et al; Phys. Lett. 86B (1979) 215.

[4] R.L. Golden et al., Phys. Rev. Lett. 43 (1979) 1196.

[5] M.A.Hasan et al., Nucl. Instr. and Meth. A295 (1990)73.

[6] P.S.Gregory et al., Nucl. Phys. B119(1977)60; A.J.Simmons et al., Nucl. Phys. B172(1980)285; D.R.Ward et al., Nucl. Phys. B172(1980)302.

[7] H.Braun et al., Proc. 5th European Symp. on Nucleon Antinucleon int., Bressanone, 1980.

[8] R. Brun et al; CERN Data Handling Division, DD/EE/84-1, CERN-CN, CH-1211 Geneva 23, Switzerland.

Table 1: Efficiencies and limits on $\tau_{\bar{p}}$ /BR for five decay modes of the antiproton. The uncertainties on the calculated ε are statistical and systematic respectively.

MODE	ε	LIMIT (95% C.L.)
$\bar{p} \rightarrow e^- + \gamma$	$(6.95 \pm 0.33 \pm 0.09) \times 10^{-4}$	1848 years
$\bar{p} \rightarrow e^- + \pi^0$	$(2.19 \pm 0.20 \pm 0.07) \times 10^{-4}$	554 years
$\bar{p} \rightarrow e^- + \eta$	$(7.00 \pm 0.77 \pm 0.40) \times 10^{-5}$	171 years
$\bar{p} \rightarrow e^- + K_S^0$	$(1.27 \pm 0.23 \pm 0.07) \times 10^{-5}$	29 years
$\bar{p} \rightarrow e^- + K_L^0$	$(4.6 \pm 1.4 \pm 0.2) \times 10^{-6}$	9 years

Figure Captions

Fig. 1 Experimental setup: (a) side view, and (b) calorimeter face showing the cell structure and cell groupings into six trigger sectors.

Fig. 2 Energy distributions: (a) calorimeter total energy distribution, and (b) distribution of calorimeter cell energies. Data (points) are compared with predictions from the beam-gas Monte Carlo simulation (histogram).

Fig. 3 Distributions of (a) cluster multiplicity, and (b) energy imbalance as defined in the text. The data (points) are compared with the beam-gas Monte Carlo predictions (histogram).

Fig. 4 Calorimeter energy distributions (points) compared with Monte Carlo predictions for $\bar{p} \rightarrow e^- \pi^0$ decay for (a) events passing a loose energy balance requirement, and (b) events with two clusters and energy imbalance $S < 0.1$ (Note: there is an overflow of one event).

(a)

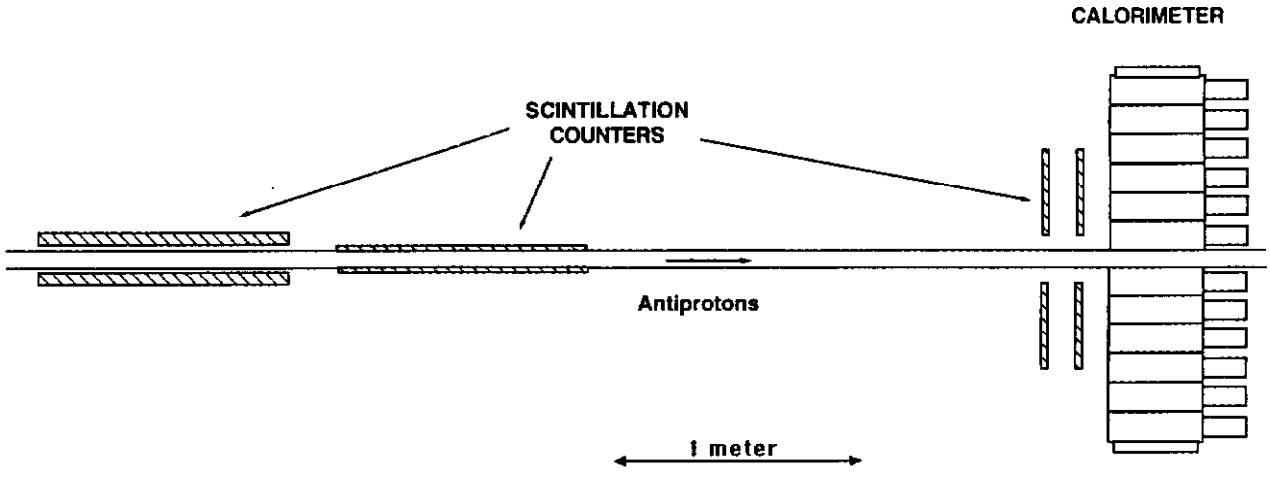

(b)

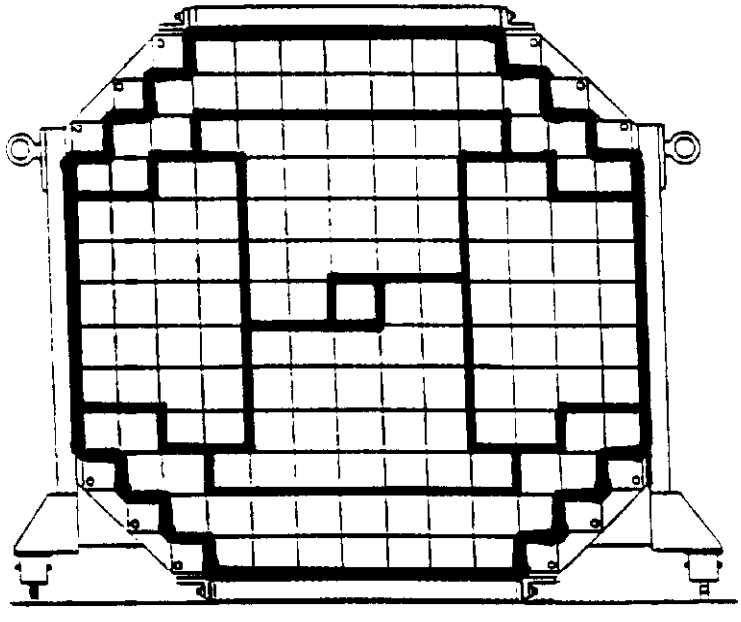

Figure 1

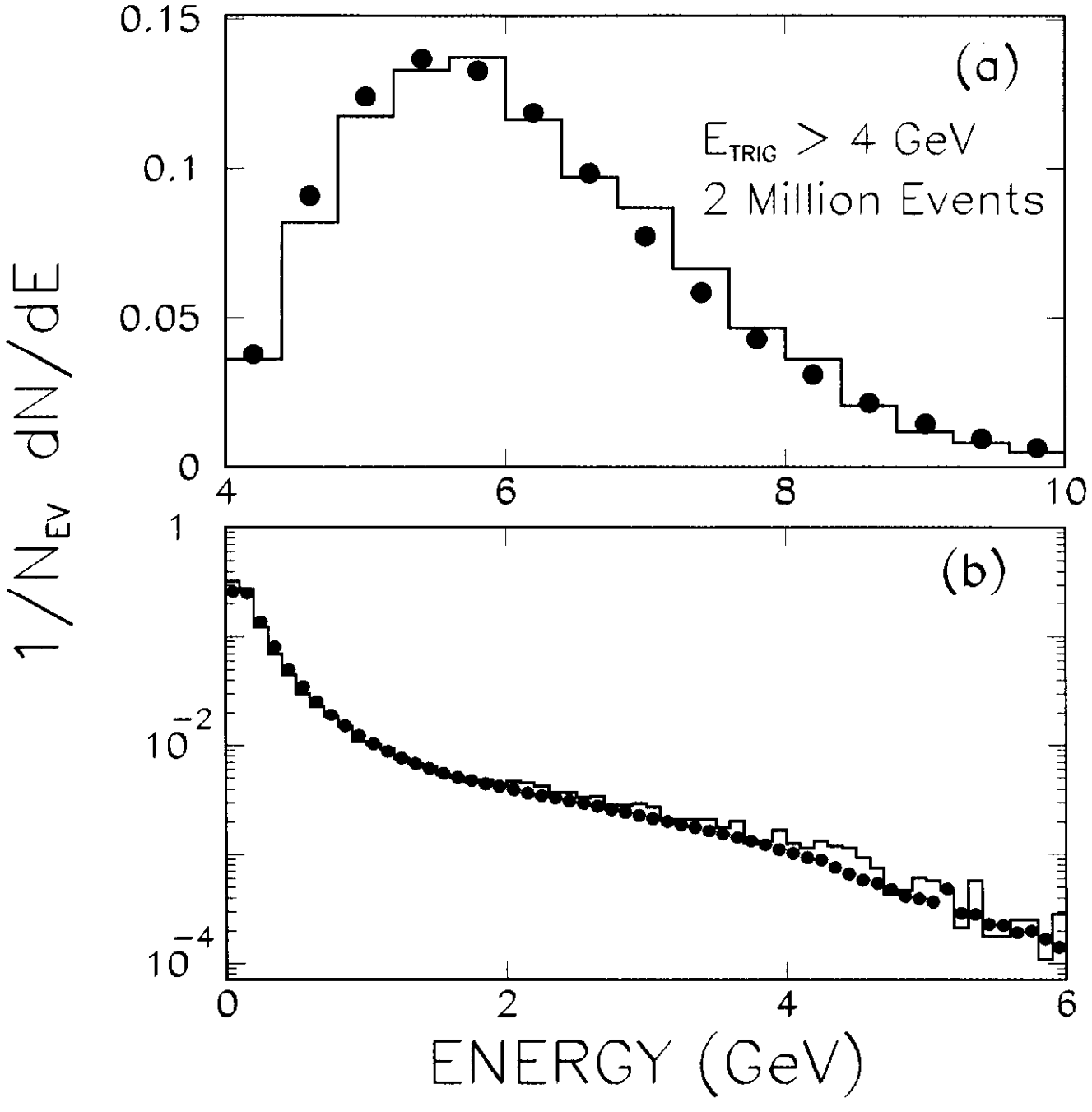
0.15
0.1
0.05
0
(a)
E_{TRIG} > 4 GeV
2 Million Events
4
6
8
10
1
10^{-2}
10^{-4}
(b)
0
2
4
6
$1/N_{EV}$ dN/dE
ENERGY (GeV)

Figure 2

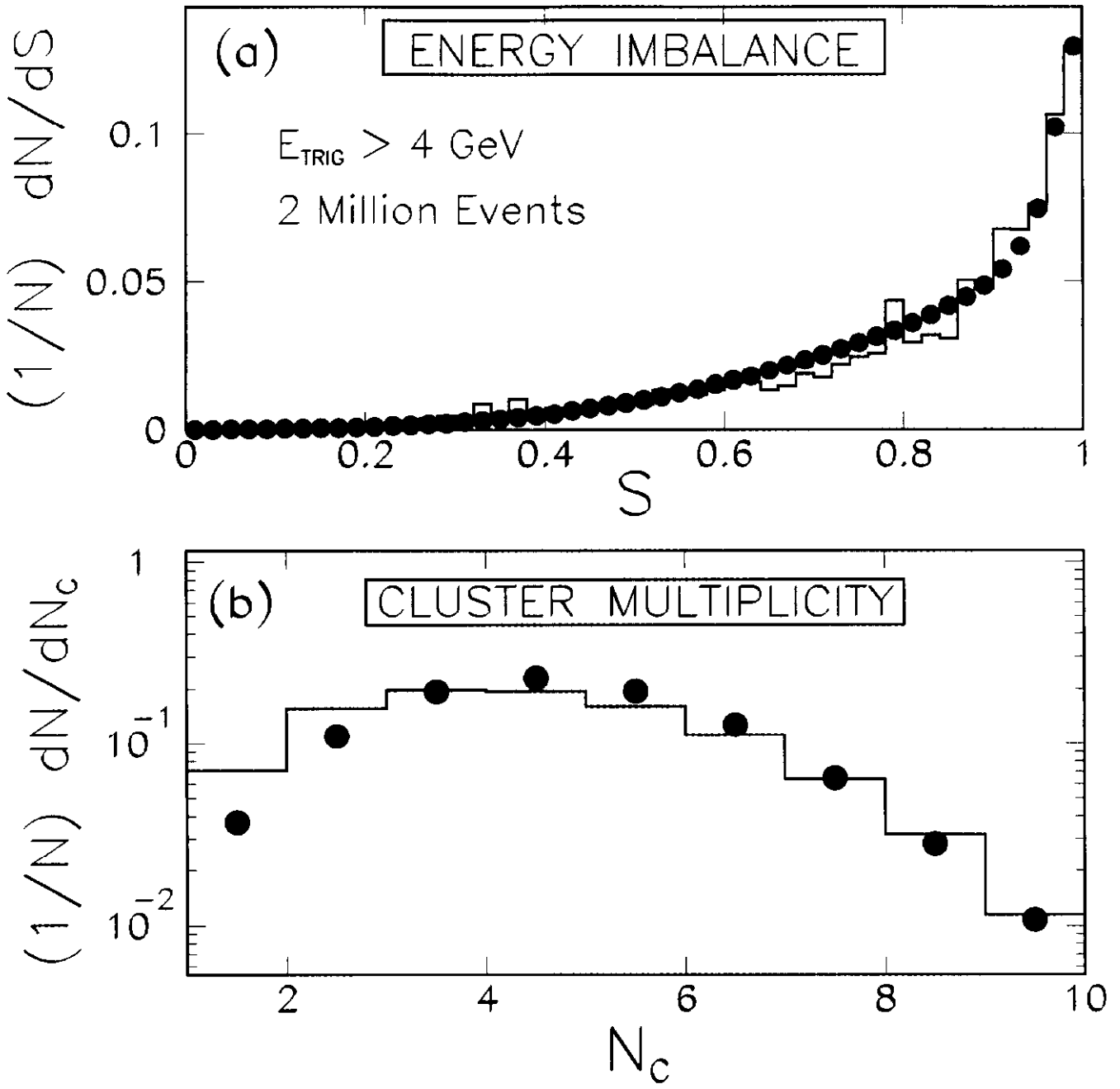
(a)
ENERGY IMBALANCE
E_{TRIG} > 4 GeV
2 Million Events
(1/N) dN/dS
S
(b)
CLUSTER MULTIPLICITY
(1/N) dN/dN$_c$
N$_c$

Figure 3

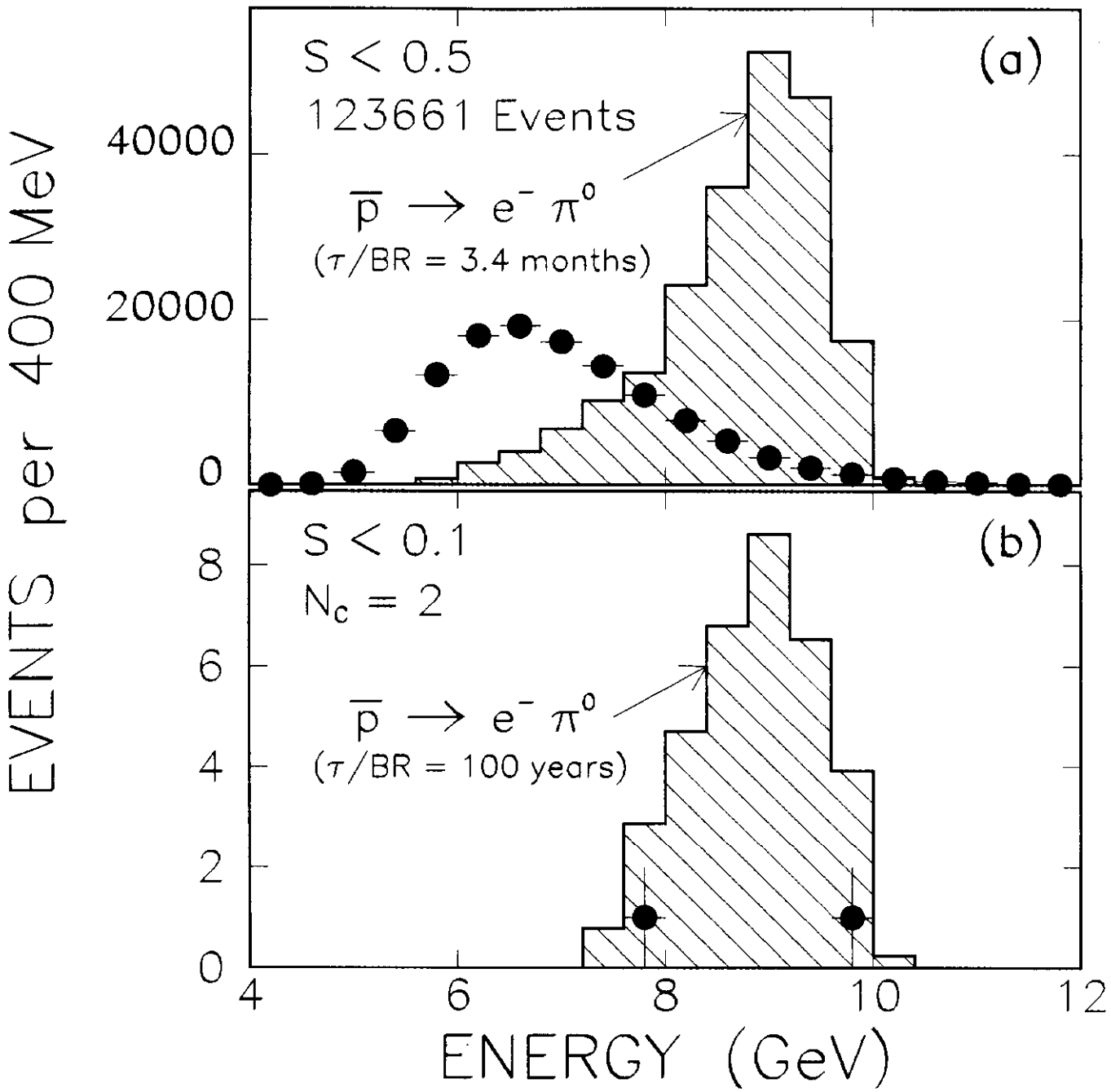
S < 0.5
123661 Events
(a)
$\bar{p} \rightarrow e^- \pi^0$
(τ/BR = 3.4 months)
40000
20000
0
S < 0.1
N_c = 2
(b)
$\bar{p} \rightarrow e^- \pi^0$
(τ/BR = 100 years)
8
6
4
2
0
4
6
8
10
12
EVENTS per 400 MeV
ENERGY (GeV)

Figure 4